# Anharmonic effects in IR, Raman, and Raman optical activity spectra of alanine and proline zwitterions

Petr Daněček
*Institute of Organic Chemistry and Biochemistry, Academy of Sciences, Flemingovo náměstí 2, 16610 Prague 6, Czech Republic and Institute of Physics, Faculty of Mathematics and Physics, Charles University, Ke Karlovu 5, 12116 Prague 2, Czech Republic*

Josef Kapitán
*Institute of Organic Chemistry and Biochemistry, Academy of Sciences, Flemingovo náměstí 2, 16610 Prague 6, Czech Republic*

Vladimír Baumruk
*Institute of Physics, Faculty of Mathematics and Physics, Charles University, Ke Karlovu 5, 12116 Prague 2, Czech Republic*

Lucie Bednárová
*Institute of Organic Chemistry and Biochemistry, Academy of Sciences, Flemingovo náměstí 2, 16610 Prague 6, Czech Republic*

Vladimír Kopecký, Jr.
*Institute of Physics, Faculty of Mathematics and Physics, Charles University, Ke Karlovu 5, 12116 Prague 2, Czech Republic*

Petr Bouř[a)]
*Institute of Organic Chemistry and Biochemistry, Academy of Sciences, Flemingovo náměstí 2, 16610 Prague 6, Czech Republic*

(Received 23 February 2007; accepted 17 April 2007; published online 13 June 2007)

The difference spectroscopy of the Raman optical activity (ROA) provides extended information about molecular structure. However, interpretation of the spectra is based on complex and often inaccurate simulations. Previously, the authors attempted to make the calculations more robust by including the solvent and exploring the role of molecular flexibility for alanine and proline zwitterions. In the current study, they analyze the IR, Raman, and ROA spectra of these molecules with the emphasis on the force field modeling. Vibrational harmonic frequencies obtained with 25 *ab initio* methods are compared to experimental band positions. The role of anharmonic terms in the potential and intensity tensors is also systematically explored using the vibrational self-consistent field, vibrational configuration interaction (VCI), and degeneracy-corrected perturbation calculations. The harmonic approach appeared satisfactory for most of the lower-wavelength (200–1800 $cm^{-1}$) vibrations. Modern generalized gradient approximation and hybrid density functionals, such as the common B3LYP method, provided a very good statistical agreement with the experiment. Although the inclusion of the anharmonic corrections still did not lead to complete agreement between the simulations and the experiment, occasional enhancements were achieved across the entire region of wave numbers. Not only the transitional frequencies of the C–H stretching modes were significantly improved but also Raman and ROA spectral profiles including N–H and C–H lower-frequency bending modes were more realistic after application of the VCI correction. A limited Boltzmann averaging for the lowest-frequency modes that could not be included directly in the anharmonic calculus provided a realistic inhomogeneous band broadening. The anharmonic parts of the intensity tensors (second dipole and polarizability derivatives) were found less important for the entire spectral profiles than the force field anharmonicities (third and fourth energy derivatives), except for a few weak combination bands which were dominated by the anharmonic tensor contributions. © *2007 American Institute of Physics*. [DOI: 10.1063/1.2738065]

## I. INTRODUCTION

The spectroscopy of the Raman optical activity (ROA) has significantly advanced for the past decade due to improvements of the instrumentation as well as development of the simulation techniques.[1,2] The ability of chiral molecules to scatter differently left- and right-circularly polarized light was first predicted by Barron and Buckingham[3] and it was soon confirmed experimentally.[4] Since then, the potential of ROA has been widely recognized and the technique successfully applied for a large number of small chiral molecules,[5] protein and nucleic acid biopolymers, and even for viruses.[5,6] Although useful information can already be obtained on an

[a)]Electronic mail: bour@uochb.cas.cz

 

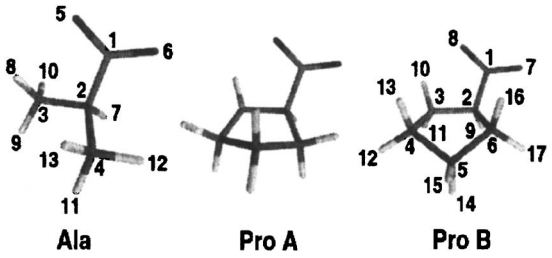


FIG. 1. L-alanine and L-proline zwitterions. The A and B proline conformers have approximately the same energy and equal populations in aqueous solutions at room temperature (Ref. 10). In the potential energy scans, the angles $\varphi=\angle(9,3,2,1)$ and $\psi=\angle(3,2,1,5)$ for alanine and the ring torsion angles of proline were varied. For the latter molecule, the angles were recalculated to the pseudorotation coordinates $P$, $\theta_m$ as defined in Ref. 10.

empirical basis comparing marker bands and characteristic features for similar structures,[7,8] it is generally accepted that only precise *ab initio* computations provide reliable basis for complete interpretation of the experiment.

The theoretical modeling often becomes quite complex and requires careful consideration of many contributions, such as conformational equilibria,[9] solvent-solute interactions, and molecular flexibility.[2,10] In the current study, in order to improve the accuracy of the simulations, we concentrate on the force field and limitations of the harmonic approximation. The analyzed spectra of proline and alanine zwitterions reported previously[2,10] serve as typical examples of molecules that are conveniently explored by ROA, particularly as good models of peptides, proteins, and other polar biopolymers. The anharmonic corrections represent relatively minor, but visible contribution. According to our knowledge, anharmonic effects in ROA spectra have not been systematically investigated yet.

Anharmonic effects in vibrational spectroscopy were often ignored or included in empirical corrections, such as the scaling constants for harmonic force fields.[11,12] Alternatively, simplified fields were proposed for this purpose.[13,14] Only for small molecules accurate potential energy surfaces can be obtained, for example, via single-point calculations at selected geometries around the equilibrium and an interpolation.[15] This approach is particularly useful when only a limited number of strongly anharmonic vibrational modes can be considered.[16] In this study we follow a more frequent method based on Taylor potential series near the equilibrium geometry.[17] The solution of the vibrational problem beyond the harmonic approximation becomes quite tedious as the motion of many degrees of freedom cannot be separated into independent coordinates.[18] Most general methods tackling this problem are based on the variational principle and involve plain vibrational configuration interaction (VCI),[19–21] vibrational coupled cluster (VCC),[22] or vibrational self-consistent field (VSCF).[19,20,23] More advanced approximations combine several approaches [e.g., VSCF and CI (Ref. 20)] or explore the perturbation theory.[24] As discussed previously, such approximate solvers of the anharmonic Schrödinger equation may not provide same solutions and are even differently sensitive to inaccuracies in the vibrational potential.[25] A particular problem in bigger molecules stems from an increased number of the harmonic vibrational states that have nearly same energies. This degeneracy, conventionally called "random" for low-symmetry systems, prevents to apply standard perturbational techniques directly to the harmonic Hamiltonian. Thus the second-order perturbation formula, for example, has to be adapted before it becomes usable for systems with the degeneracies.[25,26]

The theoretical basis of the calculations is briefly reviewed at Sec. II in the current work. In order to explore the limits of the harmonic approach the alanine and proline Raman and ROA spectra are simulated with 25 different density functional theory (DFT) potentials and compared to the experiment. Then we apply various VSCF, perturbational, and VCI anharmonic methods to the zwitterionic force fields and test their performance against experimental Raman frequencies. Finally, the anharmonic calculus is used for modeling of the vibrational frequencies and IR, Raman, and ROA spectral intensities; the significance of the anharmonic corrections is discussed in light of the approximation errors, band broadening stemming from the Boltzmann averaging, and molecular flexibility.

## II. METHOD

### A. Experiment

The backscattered Raman and incident circular polarization ROA spectra of both L and D enantiomers of proline and alanine were recorded on our spectrometer located at the Institute of Physics, as described in detail elsewhere.[2,10] The laser excitation wavelength was 514.5 nm, with a laser power of 440 mW, a spectral resolution of 6.5 $cm^{-1}$, and acquisition times of 6 and 9 h for the $H_2O$ and $D_2O$ measurements, respectively. Aqueous ($H_2O$) solutions with final concentrations of about 3 mol/l were prepared with deionized water; $D_2O$ solutions (2 mol/l) were prepared from doubly lyophilized samples. The solution Raman spectra were remeasured over a broader wave number range including the hydrogen stretching regions on a LabRam HR800 Raman microspectrometer (Horiba Jobin Yvon). A continuous Kiefer scanning mode was used with a 600 grooves/mm grating, a liquid-nitrogen-cooled charge coupled device (CCD) detector ($1024\times256$ pixels), a spectral resolution of about 4 $cm^{-1}$ (varying within the spectral range of frequencies recorded simultaneously), and a 632.8 nm laser excitation wavelength. The IR spectra of both compounds (about 10% aqueous solutions) were recorded on a Vectra 33 Fourier transform infrared spectrometer (Bruker) using a single reflection diamond horizontal attentuated reflection (HATR) accessory (Pike Technologies).

### B. Anharmonic corrections

A simplified potential expansion in the vibrational normal mode coordinates $\{Q_i\}$ was used,

TABLE I. Comparison of the harmonic vibrational frequencies of alanine and proline calculated at 25 approximation levels to experimental Raman and ROA data. The CPCM solvent model and 6-31++G** basis set were used in the modeling. Slopes ($a$), standard deviations [$\Delta(\omega_{calc}-\omega_{expt})$], and dispersions [$\delta(\omega_{calc}-a\omega_{expt})$] are given for a linear fit to experimental wave numbers within 200–1800 $cm^{-1}$. Methods giving best Raman and ROA intensity profiles (judged subjectively by visual comparison to experiment) are marked by the asterisk ( * ).

| | Alanine in $H_2O$ | | | Proline in $H_2O$ | | | Proline in $D_2O$ | | |
|---|---|---|---|---|---|---|---|---|---|
| Method[a] | $a$ | $\Delta$ | $\delta$ | $a$ | $\Delta$ | $\delta$ | $a$ | $\Delta$ | $\delta$ |
| HF | 1.088 | 104 | 28 | 1.092 | 101 | 19 | 1.089 | 96 | 22 |
| BHandHLYP* | 1.042 | 53 | 23 | 1.046 | 51 | 14 | 1.043 | 48 | 18 |
| MP2 | 1.018 | 32 | 24 | 1.021 | 27 | 16 | 1.018 | 27 | 20 |
| MPW1PW91* | 1.006 | 17 | 16 | 1.012 | 19 | 14 | 1.009 | 19 | 17 |
| B1LYP | 1.004 | 24 | 24 | 1.008 | 17 | 15 | 1.004 | 20 | 19 |
| B3P86* | 0.999 | 16 | 16 | 1.006 | 15 | 14 | 1.002 | 17 | 17 |
| B3PW91* | 0.999 | 17 | 17 | 1.005 | 15 | 14 | 1.001 | 17 | 17 |
| *PBE1PBE** | 1.004 | 15 | 15 | 1.002 | 19 | 19 | 1.004 | 22 | 22 |
| B98* | 0.998 | 21 | 20 | 1.002 | 16 | 16 | 0.998 | 19 | 19 |
| B3LYP* | 0.997 | 21 | 21 | 1.001 | 15 | 15 | 0.997 | 19 | 19 |
| *HCTH* | 0.983 | 27 | 18 | 0.989 | 19 | 15 | 0.994 | 19 | 18 |
| *HCTH147* | 0.978 | 32 | 20 | 0.984 | 24 | 15 | 0.979 | 29 | 19 |
| *VSXC* | 0.977 | 37 | 26 | 0.980 | 26 | 15 | 0.975 | 32 | 19 |
| OLYP | 0.974 | 36 | 21 | 0.980 | 28 | 17 | 0.976 | 32 | 20 |
| *LSDA* | 0.976 | 43 | 33 | 0.975 | 37 | 25 | 0.971 | 38 | 23 |
| *BPW91* | 0.965 | 45 | 20 | 0.971 | 35 | 15 | 0.967 | 40 | 19 |
| *BPW91*[b] | ⋯ | ⋯ | ⋯ | 0.966 | 40 | 14 | 0.962 | 44 | 18 |
| *BPW91*[c] | ⋯ | ⋯ | ⋯ | 0.971 | 34 | 13 | 0.967 | 39 | 18 |
| SVWN5 | 0.972 | 45 | 31 | 0.971 | 40 | 24 | 0.968 | 40 | 22 |
| *PW91PW91* | 0.964 | 45 | 18 | 0.970 | 35 | 14 | 0.966 | 39 | 18 |
| *G96LYP* | 0.963 | 49 | 25 | 0.968 | 39 | 19 | 0.964 | 45 | 23 |
| *BLYP* | 0.960 | 52 | 26 | 0.965 | 42 | 19 | 0.960 | 48 | 23 |
| *BP86* | 0.961 | 49 | 19 | 0.964 | 45 | 22 | 0.962 | 43 | 18 |
| *PW91LYP* | 0.960 | 51 | 23 | 0.964 | 43 | 17 | 0.959 | 48 | 22 |
| *PBELYP* | 0.958 | 53 | 24 | 0.963 | 43 | 17 | 0.958 | 49 | 22 |

[a]GGA functionals are written *in italic*.
[b]AUG-cc-PVDZ basis.
[c]AUG-cc-PVTZ basis.

$$V(Q_1,\ldots,Q_M)=\sum_{i=1}^{M}\frac{\omega_i^2}{2}Q_i^2+\frac{1}{6}\sum_{i=1}^{M}\sum_{j=1}^{M}\sum_{k=1}^{M}c_{ijk}Q_iQ_jQ_k+\frac{1}{24}\sum_{i=1}^{M}\sum_{j=1}^{M}\sum_{k=1}^{M}\sum_{l=1}^{M}d_{ijkl}Q_iQ_jQ_kQ_l+\cdots, \quad (1)$$

while the rotation-vibration coupling was neglected. Only semidiagonal normal mode quartic constants with two and more identical indices (e.g., $d_{ijkk}$) were considered, obtained from semidiagonal Cartesian quartic constants; $\{\omega_i\}$ are the harmonic frequencies and $M=3\times$number of atoms$-6$. For the solution of the anharmonic problem the VCI, VSCF, and the second-order perturbation theory (PT2) were used as described in detail elsewhere and implemented in our program GVIB.[25] In the VCI calculations 1000–6000 harmonic oscillator basis functions were included, which contained at most five excitations. In the VSCF method[19] one-dimensional Schrödinger equations,

$$\left(-\frac{1}{2}\frac{\partial^2}{\partial Q_i^2}+v_i(Q_i)\right)\psi_i(Q_i)=e_i\psi_i(Q_i), \quad (2)$$

were solved iteratively until changes of the energies $e_i$ were smaller than $10^{-6}$ $cm^{-1}$. The self-consistent averaged potentials are defined as $v_i(Q_i)=\langle\Pi_{j=1,j\neq i}^{M}\psi_j(Q_j)|V(Q_1,\ldots,Q_M)|\Pi_{k=1,k\neq i}^{M}\psi_k(Q_k)\rangle$. As described previously,[25] the potentials can be averaged either using the ground state only or with appropriate excited states. These two approaches are referred to as gVSCF and eVSCF, respectively.

A perturbational calculus was applied to the harmonic (referred to as PT2/Harm) as well as to the VSCF solutions (PT2/VSCF).[24] In both cases, a modified second-order perturbational formula was used, as it previously provided superior results to the conventional approach, especially for systems with nearly degenerate energy levels.[25] Specifically, the second-order correction to the energy of a state $n$ was obtained as

$$E_n^{(2)}=\tfrac{1}{2}\sum_{m\neq n}[E_m-E_n+W_{mm}-W_{nn}\pm\sqrt{(E_m-E_n+W_{mm}-W_{nn})^2+4|W_{nm}|^2}], \quad (3)$$

where the + sign holds for $E_n>E_m$ and − sign for $E_n<E_m$. $\{E_n\}$ are the unperturbed energies and $W_{nm}=\langle n|W|m\rangle$ is the perturbation potential matrix element.

Incident circular polarized backscattering Raman and ROA intensities as well as the IR absorption were obtained for each method with corresponding vibrational wave func-

TABLE II. rms deviations ($cm^{-1}$) between the experimental and calculated alanine and proline frequencies within 200-1800 $cm^{-1}$; nine levels of the vibrational problem are compared. By default, three (five for BPW91) lowest-frequency states of alanine and six of proline were ignored.

| | Alanine | | | Proline |
|---|---|---|---|---|
| Vibrational approximation | Electronic level B3LYP/6-31++G** | B3LYP/6-311++G** | BPW91/6-31++G** | B3LYP/6-31++G** |
| Harmonic | 21 | 20 | 45 | 15 |
| gVSCF | 31 | 34 | 69 | 25 |
| eVSCF | 34 | 37 | 72 | 25 |
| gVSCF+PT2 | 50 | 54 | 89 | 41 |
| eVSCF+PT2 | 54 | 56 | 90 | 42 |
| Harm+PT2 | 50 | 53 | 86 | 40 |
| Harm+VCI[a] | 18 | 17 | 34 | 24 |
| Harm+VCI[b] | 33 | ··· | ··· | 30[d] |
| Harm+VCI[c] | 29 | 18 | ··· | 32 |

[a]1000 VCI states.
[b]1000 VCI states, one mode ignored.
[c]6000 VCI states.
[d]Four modes ignored.

tions using general formulas that can be found elsewhere.[27,28] For PT2 frequencies the harmonic intensities were used in spectral plots.

### C. Computations

Alanine and proline equilibrium geometries (see Fig. 1 for the lowest-energy alanine and two proline conformers) and harmonic force fields were obtained with the aid of the GAUSSIAN program[29] using 25 different levels of electronic theory including the HF,[30] MP2,[31] BHandHLYP,[32] MPW1PW91,[33] B1LYP,[34] B3P86,[35,36] B3PW91,[35,37] PBE1PBE,[38] B98,[39] B3LYP,[35] HCTH,[40] HCTH147,[40] VSXC,[41] OLYP,[42] LSDA,[43] BPW91,[32,37] SVWN5,[44] PW91PW91,[45] G96LYP,[46,47] BLYP,[47] BP86,[36] PW91LYP,[47] and PBELYP[38] DFT functionals, mostly with the 6-31++G** basis set and the CPCM ("COSMO-PCM")[48] solvent model. Raman intensities were calculated at the same level. For computation of the anharmonic corrections (third and fourth energy derivatives, second tensor derivatives) the B3LYP/6-31++G** method was used by default, with occasional utilization of the BPW91 and PW91PW91 functionals and smaller 6-31+G** and 6-31G** basis sets. Basis sets of similar quality appeared satisfactory for ROA spectra previously.[49]

The anharmonic constants were calculated by numerical differentiation with a displacement of 0.025 Å. Control computations with steps within 0.005–0.075 Å provided similar results. Occasionally, individual anharmonic constants were calculated unrealistically high, which was attributed to an unstable CPCM model implementation. In control computations molecular CPCM cavities were both fixed at the optimized geometry and allowed to follow displaced nuclei during the differentiation. As both approaches gave very similar vibrational frequencies, the default Gaussian procedure (with the cavity displacement) was used further on. Raman and ROA spectra were simulated using the GVIB program and the theory described above, with Lorentzian bands $\Delta=6.5$ $cm^{-1}$ wide (full width at half height). Contribution of each transition of frequency $\omega_i$ to the spectrum was thus

$$S(\omega)=I\left[1-\exp\left(-\frac{\omega_i}{kT}\right)\right]^{-1}\frac{1}{\omega_i}\left[4\left(\frac{\omega-\omega_i}{\Delta}\right)^2+1\right]^{-1},$$

where $I=6(7\alpha_{ij}\alpha_{ij}+\alpha_{ii}\alpha_{ii})$ for Raman and $I=(48/c)(3\alpha_{ij}G'_{ij}-\alpha_{ii}G'_{jj}+\omega_{exc}\varepsilon_{ijk}\alpha_{il}A_{jkl}/3)$ for ROA backscattered intensities, where $\omega_{exc}$ is the laser light frequency, $T$ temperature (298 K), and $k$ the Boltzmann constant; $\boldsymbol{\alpha}$, $\mathbf{G}'$, and $\mathbf{A}$ are the electric dipole–electric dipole, magnetic dipole–electric dipole, and electric quadrupole–electric dipole polarizability normal mode derivatives.[27] For absorption spectra the same Lorentzian shapes were used without any temperature correction. 0–5 lowest-energy modes were not included in the anharmonic corrections in order to avoid numerical instabilities. Supposedly, their coupling to the higher-frequency modes is small and their influence on the spectra can be partially accounted to by the Boltzmann averaging as discussed below.

## III. RESULTS AND DISCUSSION

### A. The harmonic limit

In the past the harmonic approximation has been established as an effective and surprisingly accurate approximation for interpreting vibrational spectra of most molecules.[18,50] This appears to be also the case for the proline and alanine zwitterions. The precision of the harmonic nuclear potential, however, depends strongly on the electronic approximation level and modeling of the environmental factors. Also, one has to realize that atoms may move in an effective harmonic well while other effects are averaged out. For example, the zwitterions would not exist in vacuum and the solvent needs to be added at the electronic computations. Fortunately, the CPCM continuum model used in this study provides reasonable frequencies for the two amino acids in aqueous solutions.[2,10]

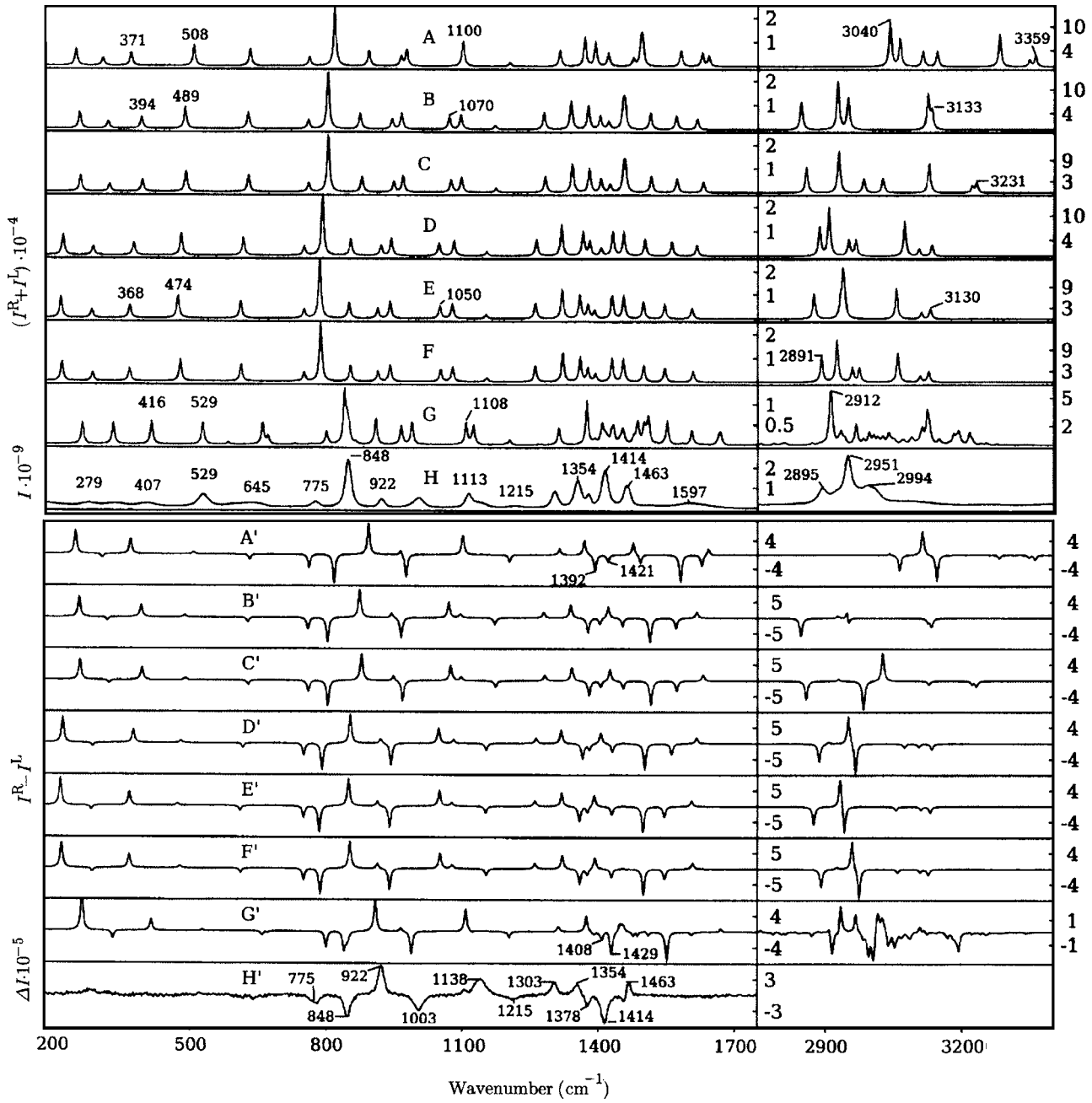


FIG. 2. Raman (A–H) and ROA (A′–H′) spectra of L alanine: comparison of the harmonic (A and A′), eVSCF (B and B′), gVSCF (C and C′), PT2 (D and D′), PT2/eVSCF (E and E′), PT2/gVSCF (F and F′), and VCI (G and G′, with 5000 harmonic oscillator basis functions) calculations with the experiment (H and H′). The B3LYP/CPCM/6-31++$G^{**}$ force field and polarizability derivatives were used in all calculations, three low-frequency modes were ignored. The $y$ scale is arbitrary for the simulations, while for experiment it corresponds to the number of counts on the CCD detector. The absolute scale does not apply to the high-frequency part of the Raman spectrum (>2500 $cm^{-1}$, trace H) which was measured separately on the microscope.

Systematic improvement of the DFT electronic methods is difficult. On the other hand, they are often the only computationally feasible alternatives for bigger systems. Under these circumstances, we find it important to test their performance at least statistically. Particularly, in Table I, we compare systematic and root mean square errors for alanine and proline vibrational frequencies within 200–1800 $cm^{-1}$ as obtained by 25 approximation levels. In this comparison, we neglect the anharmonic effects and calibrate the computational methods against the experimental values directly. At the same time, the band assignments were verified by visual comparison of experimental and simulated spectral intensities.

Generally, the approximations to the electronic problem summarized in Table I provide similar errors as observed previously for other molecules in vacuum.[12,51] On average the present calculations are closer to the experiment, because of the solvent correction and the exclusion of the high-frequency vibrations from the statistics. The HF method still overestimates the frequencies most significantly, by about 9% for both amino acids (see the slope $a$ of the fit). At the other extreme, most of the "pure" generalized gradient approximation (GGA) functionals underestimate the frequencies, up to by ~4% for the PW91LYP and PBELYP methods. Not surprisingly, the "mixed" functionals containing both the HF nonlocal and the GGA local (density-dependent)

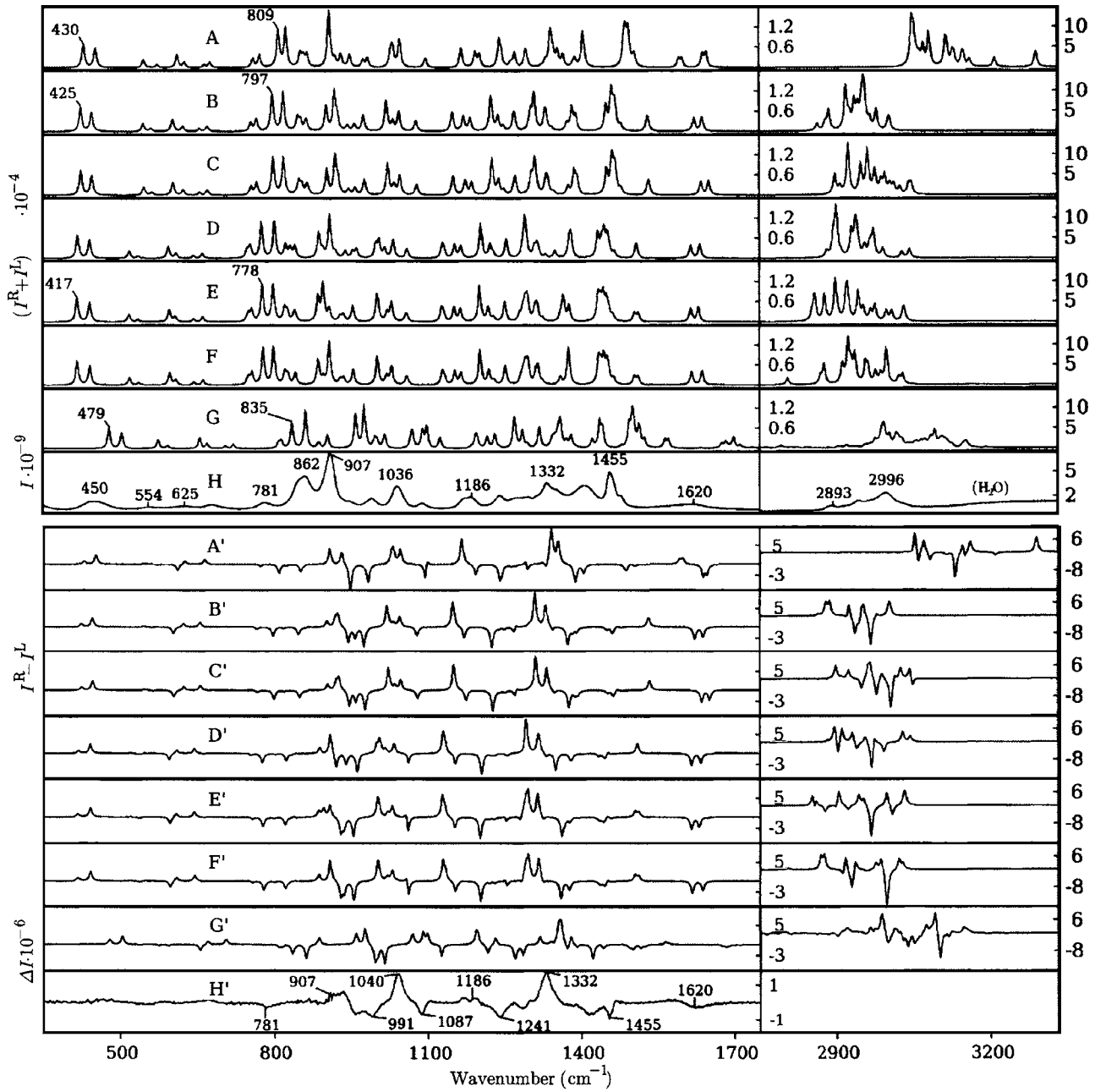


FIG. 3. Raman (A–H) and ROA (A′–H′) spectra of L proline: comparison of the harmonic (A and A′), eVSCF (B and B′), gVSCF (C and C′), PT2 (D and D′), PT2/eVSCF (E and E′), PT2/gVSCF (F and F′), and VCI (G and G′, with 5000 harmonic oscillator basis functions) calculations with the experiment H and H′). The B3LYP/CPCM/6-31++$G^{**}$ force field and polarizability derivatives were used for all calculations, five lowest wave number modes were ignored.

energy term, such as B3LP or B3PW91, thus provide the best results. Note that the slope of the fit ($a$) often differs from one by ~0.1% only. Nevertheless, some pure GGA functionals missing the HF exchange terms, such as HCTH or PBE1PBE, perform very well, too, and may be favored in applied computations because of their lesser demands on computer CPU time and memory. Previously, we and others often used the BPW91 functional for simulation of the peptide and protein vibrational circular dichroism (VCD), as it provided better amide I frequencies (C═O stretch) with more modest computational demands than the more frequent B3LYP.[52] Although the BPW91 method also provides reasonable Raman and ROA spectral shapes (not shown) for the zwitterions, the vibrational frequencies are too low. Thus application of this functional to the Raman spectra comprising a wide range of transitions does not appear as advantageous as for VCD.

We can also see that it is the treatment of the correlation energy, not the exchange, that most significantly improves the HF results: the MP2 perturbation correlation treatment reduces the HF error significantly. However, for the DFT techniques, a more detailed discussion of the contribution of the exchange and correlation parts is not meaningful due to the empirical and often complicated mathematical form of the functionals. More importantly, previous experience suggests[2,10] that even the functionals providing the best fre-

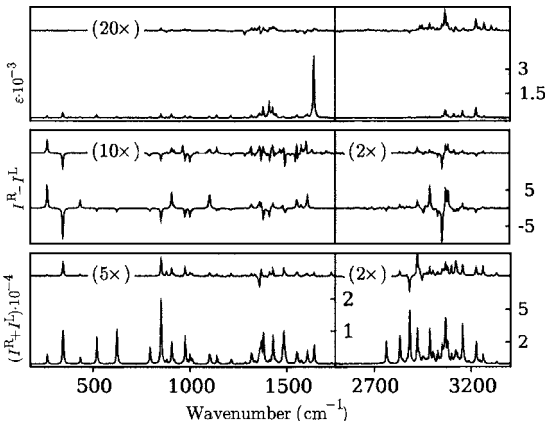


FIG. 4. Absorption (top), ROA (middle), and Raman (bottom) alanine spectral intensities with the second dipole and polarizability derivative contributions. The contributions are magnified and plotted separately above the spectra as simulated by the VCI method (1000 basis functions, three ignored modes).

quencies and Raman and ROA spectral profiles [e.g. those indicated by the asterisk ( *) in Table I] could not completely explain all the experimental features. This situation may be even more problematic for bigger molecules or for regions with many overlapping bands. For such cases neither the best precision (15–20 cm$^{-1}$) achieved can lead to correct prediction of spectral band ordering and a proper assignment.

### B. Anharmonic corrections below 1800 cm$^{-1}$

For the harmonic computations we restrict ourselves to the DFT potentials, mostly the B3LYP functional, because more advanced methods become prohibitively demanding in terms of computer power. Nevertheless, we rely on the previous experience[53] indicating that the main anharmonic effects can be described by DFT practically with the same precision as with the wave-function-based electronic calculus. Inclusion of the anharmonic potential does not make automatically the agreement with the experiment better. While this is true for abstract model systems,[24] many loopholes are hidden in practical applications. Limited precision of the electronic models, such as those in Table I, probably burdens the harmonic frequencies with an error comparable to the anharmonic corrections. Similar inaccuracies may be expected in estimation of the anharmonic constants. Also, as pointed out previously, approximate solvers of the anharmonic vibrational problem are very sensitive to random errors in the potential, even when the random degeneracy problem is avoided.[25] Particular problem represents the many inaccurate terms that are summed over in the VSCF and PT2 methods.

Due to these factors the VSCF, PT, and VCI anharmonic corrections summarized in Table II do not lead to a convincing statistical improvement. The VCI computation improves the harmonic results for alanine, but only when three lowest-energy modes are ignored. An incompleteness of the VCI state space does not seem to be a problem in the lower-frequency region (<1800 cm$^{-1}$) where the state density is low. The VSCF method provides rms deviations by about 50% bigger than the harmonic limit, while the perturbation methods give a 100% increase of the deviation. Calculated harmonic and anharmonic frequencies of proline are on average closer to the experiment than for alanine; otherwise relative performance of all the vibrational methods is about the same for both molecules. Based on our previous experience[25] we suspect that the anharmonic force field inaccuracies stemming from the discrete solvent CPCM model implementation are most responsible for the errors. Apparently, the modified second-order perturbational formula (3) could eliminate sensitivity to random degeneracies, but it still at least mildly amplifies the nuclear potential inaccuracies. Thus we have to conclude that the applied methods cannot statistically improve the harmonic frequencies in the lower wave number region.

### C. Spectral intensities and the high-frequency region

However, the unconvincing improvement in the lower-frequency region does not mean that the estimation of the anharmonic part of the potential is meaningless. On the contrary, as can be seen in Figs. 2 and 3 for alanine and proline, respectively, the anharmonic computations can significantly improve not only the higher-frequency region dominated by the hydrogen stretching modes but also cause intensity redistributions in the lower-frequency region. In Figs. 2 and 3 seven approximations of the vibrational Hamiltonian (harmonic, eVSCF, gVSCF, PT2, PT2/eVSCF, PT2/gVSCF, and VCI) are compared to the solution ($H_2O$) Raman and ROA amino acid spectra. The nonvariational methods converge relatively smoothly for the transitions below 1800 cm$^{-1}$, mostly overcorrecting the harmonic results and provide frequencies too low. For example, for alanine, the harmonic $CO_2$ rocking band at 508 cm$^{-1}$ (trace A, Fig. 2) is calculated at 474 cm$^{-1}$ by the PT2 methods, while the experimental value is 529 cm$^{-1}$. The VCI computation brings the frequency back to the harmonic and experimental value, to 529 cm$^{-1}$. This is a typical behavior for both the proline and alanine spectral bands within 200–1000 cm$^{-1}$ and can also be observed, for example, for the respective harmonic/(eVSCF)PT2/VCI/experimental frequencies of CH3 wagging and C–C stretch (1100/1050/1108/1113 cm$^{-1}$) and $NC_\alpha C$ deformation modes (371/368/416/407 cm$^{-1}$) of alanine, and $CO_2$ bending (430/417/479/450 cm$^{-1}$) and ring deformation (809/778/835/862 cm$^{-1}$) of proline.

Therefore only the VCI method seems to have the potential to improve the harmonic computations in this region. For VSCF and VCI, virtually same Raman and ROA intensities are obtained for most bands as at the harmonic limit (anharmonic intensity corrections were not implemented for the PT methods). The gVSCF and eVSCF spectra (traces B, C, B′, and C′ in Figs. 2 and 3) are very similar, as are all the PT2 simulations (D–F and D′–F′). Only for the highest-frequency (N–H stretching) vibration of alanine the eVSCF and gVSCF corrections differ substantially: the former shifts the harmonic band (3359 cm$^{-1}$, trace A in Fig. 2) to 3133 cm$^{-1}$ (trace B), while the second provides a much smaller shift, to 3231 cm$^{-1}$ (trace C). The application of the second-order perturbation theory significantly changes the VSCF results, often by tens of cm$^{-1}$. In the case of the ala-

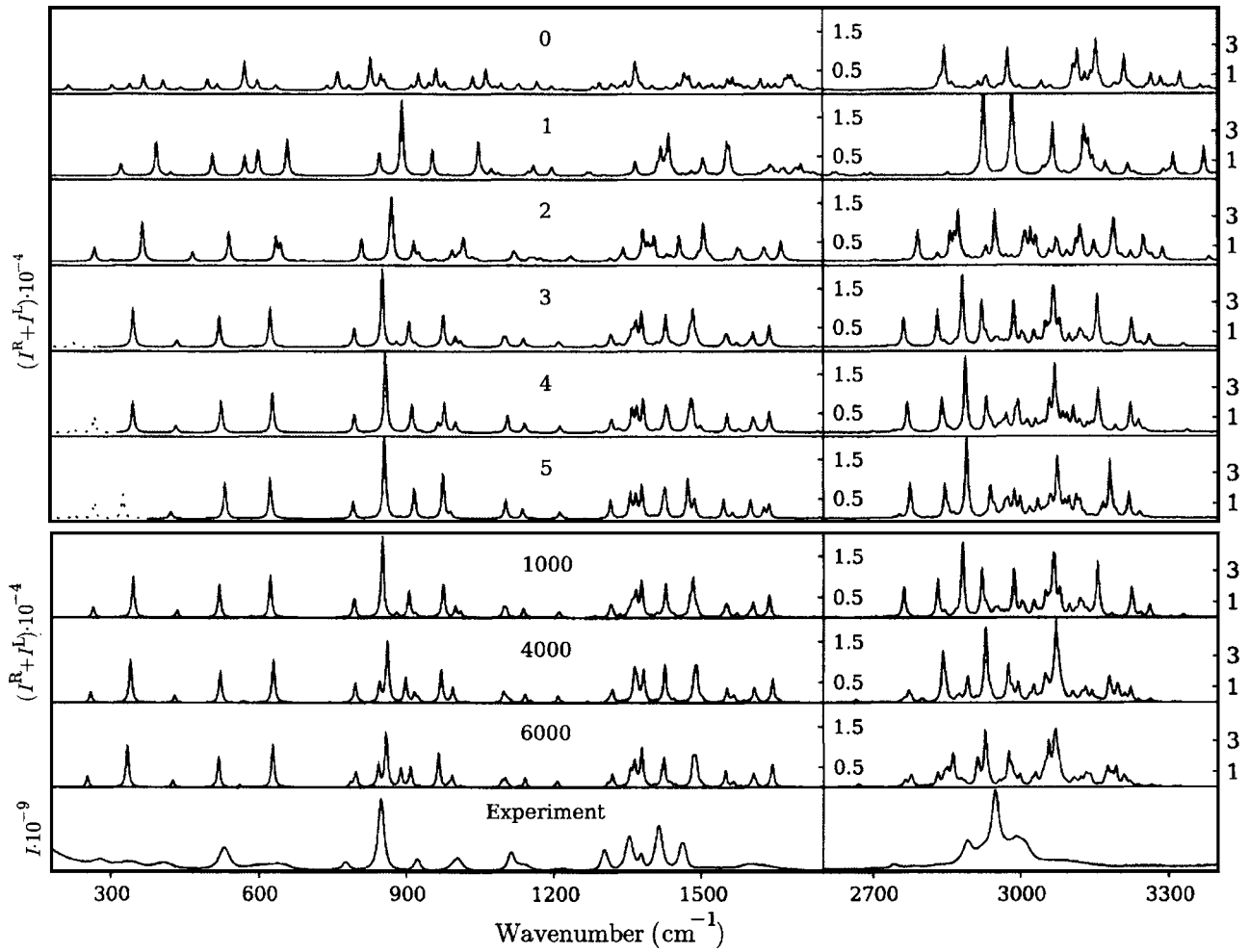


FIG. 5. Convergence of the alanine B3LYP/CPCM/6-31++$G^{**}$ VCI calculation: At the top, dependence of the Raman spectra on the number of ignored modes (written in the figure, their harmonic contributions are plotted by the dashed line) for 1000 VCI states. For three ignored modes the dependence of the spectra on the number of VCI states is plotted in the lower panel.

nine N–H stretch, for example, the PT2 corrections smooth out the gVSCF and eVSCF differences, giving approximately the same frequency (~3130 $cm^{-1}$, traces E and F in Fig. 2) if applied to both methods.

Within ~200–1200 $cm^{-1}$ the anharmonic corrections provided mostly plain frequency shifts. Within 1200–2000 $cm^{-1}$, however, even the VSCF and PT2 methods cause a visible redistribution of the Raman and ROA intensities. This region is dominated by C–H and N–H bending and C=O and C–N stretching modes, and the density of vibrational states becomes quite high. Resultant spectral shapes can thus be easily influenced by a small change of the numerical model. Again, only the VCI calculus provides a clear improvement of the harmonic spectra. For example, the relative intensities of the negative ROA alanine bands at 1392 and 1421 $cm^{-1}$ (Fig. 2, A′) are switched in VCI (G′, smaller band at 1408, deeper at 1429 $cm^{-1}$), in favor of the experiment (H′, 1378 and 1414 $cm^{-1}$). Also for proline (Fig. 3) the overall Raman and ROA profile seems to be best reproduced by the VCI simulation; however, in this case the spectra are becoming too complex to be explicable on a basis of individual transitions. Clearly, the anharmonic calculus is important and can mostly improve the spectra in the entire wave number region, but it is very difficult to obtain a band-to-band agreement for our solvated and flexible molecules. An improvement of the solvent modeling may be desirable, namely, for a better reproduction of the force field of the polar groups. This task appears presently too complex and goes beyond the scope of this study. On the other hand, the flexibility aspect can be modeled more easily and will be discussed below.

In the C–H and N–H stretching regions all the anharmonic methods improve the harmonic frequencies. For example, the lowest C–H stretching band of alanine is obtained at 3040 $cm^{-1}$ at the harmonic limit, while the 2891 and 2912 $cm^{-1}$ PT2/gVSCF and VCI peaks are much closer to the experimental value of 2895 $cm^{-1}$. The VCI method provides best Raman C–H stretching profiles, although the agreement with the experiment is far from being perfect. Unfortunately, the N–H stretching vibrations are influenced by the hydrogen bonding, very poorly reproduced by the continuum solvent model; additionally, this region is obscured by the O–H water stretching and unusable for even a qualitative analysis. Reliable experimental ROA spectra could not be obtained in this region so far.

As follows from the basic properties of the harmonic oscillator,[18] higher dipole and polarizability derivatives do not contribute to spectral intensities in harmonic systems.

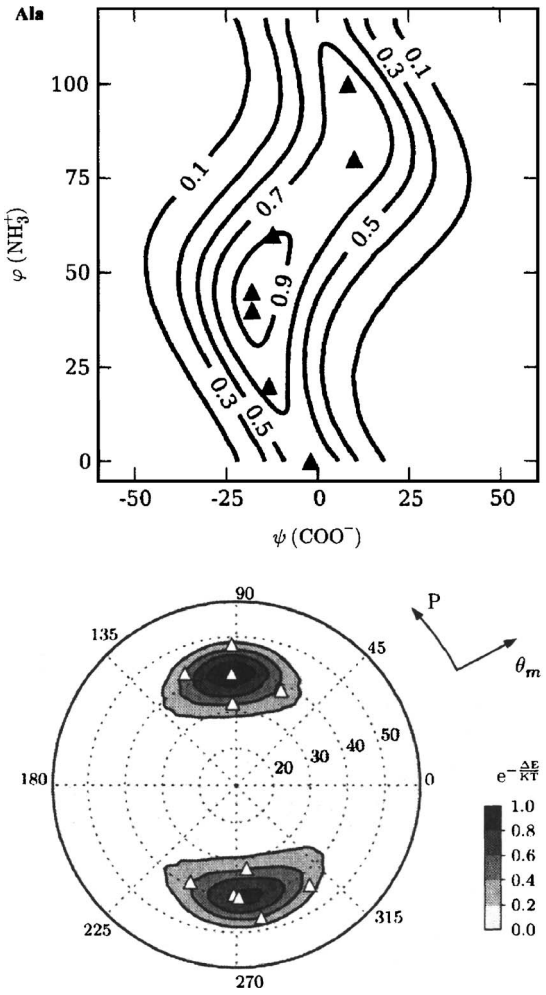


FIG. 6. Relative probability distributions of alanine (top) and proline (bottom) conformers at 300 K. For conformers marked by the triangles anharmonic IR, Raman, and ROA spectra were calculated and averaged in Figs. 7–9. (Note that the polar proline plot starts with $\theta_m = 10°$ in the center.)

Leaving this method known also as the "double-harmonic" approximation we can investigate separately anharmonic spectral corrections stemming from the force field (in the present model third and fourth energy derivatives) and the intensity tensors (second derivative of the electric dipole-electric dipole, electric dipole–magnetic dipole, and electric dipole–electric quadrupole polarizabilities[27]). As shown in Fig. 4 where the absorption, ROA, and Raman L-alanine spectra are simulated with the VCI method, the second intensity tensor derivatives constitute relatively minor contributions to total intensities. However, this term seems to be more important for Raman and ROA spectra than for the absorption. This may imply a generally increased sensitivity of the Raman spectroscopy to small geometry variations. As expected, the higher-frequency strongly anharmonic vibrations are more affected by the "intensity tensor anharmonicity" than the lower-frequency transitions. In practical terms, the inclusion of the second polarizability derivatives may be most important for improving the Raman intensities, relative ratios of which can be measured with a high precision. It is probably too small to be detectable in ROA due to the experimental noise. Similar magnitude of the tensor second derivative corrections was also observed for the proline zwitterion and is not shown in the manuscript.

### D. Error estimation and stability analyses

The limited fourth-order Taylor expansion is not suitable for representing the potential energy surface along the low-frequency normal modes, such as the rotations of methyl or carbonyl groups. The anharmonic (VSCF and VCI) methods appeared to be very sensitive to such potentials and we noticed repeatedly convergence problems, unless the lowest lying modes were ignored ("frozen"). For example, typically about three to five modes had to be frozen for alanine and six for proline before the eVSCF calculations fully converged. This freezing is partially justifiable by a limited coupling of these modes to the higher-frequency vibrations. However, the coupling cannot be *a priori* excluded. Therefore, an extension of the anharmonic treatment, at least for some low-frequency vibrations, via a Boltzmann temperature averaging will be shown below.

Nevertheless, in Fig. 5, we can see that the freezing does not affect the calculated frequencies dramatically. The influence of the anharmonic coupling of the low-frequency modes can be seen in the upper part of the figure, where the alanine Raman spectra are simulated with 0–5 ignored modes. When all modes are included, the VCI spectrum is unrealistic. Additionally, the lowest-energy state obtained by the Hamiltonian diagonalization does not correspond to the real ground state. From two ignored modes (approximately corresponding to $NH_3^+$ and $CO_2^-$ group rotations), however, the VCI spectra start to converge and inclusion/omission of the mode number 3–5 does not seem to be crucial for reproduction of the middle and high frequencies.

The ignoring of the lowest-energy modes in the anharmonic calculus also enables us to limit the number of VCI states taken in the diagonalization. Alanine Raman spectra simulated with 1000, 4000, and 6000 states (lower part of Fig. 5) appear reasonably converged within 300–3300 $cm^{-1}$. In this region of fundamental vibrations the density of vibrational states is relatively low. The amount of 6000 states (representing only 1.4% of all five-times excited states contributing to the second-order fundamental corrections), for example, thus seems to be sufficient to cover most of the coupling and diagonal anharmonic interactions. However, small intensity changes are still visible, even for the bands around 900 $cm^{-1}$. As discussed before,[25] application of the VCI method to bigger molecules will be always limited. Even when the number of the states can be somewhat increased using indirect diagonalization methods[21] (not implemented here) it is questionable if a fully converged mathematical solution exists and should be sought. Clearly, for proline and alanine the plain VCI method is not usable for the Taylor-style potential unless the lowest-energy modes are treated separately. Additionally, an involvement of all-mode coupling in VCI appears rather luxurious with respect to the physical reality, where 3–4 mode interactions usually determine the frequencies with a sufficient accuracy.[14,16,54] Therefore, for the incomplete anharmonic potentials, it appears reasonable to use the limited VCI, which comprises most of the intermode coupling and provides a first-order correction to the spectra.

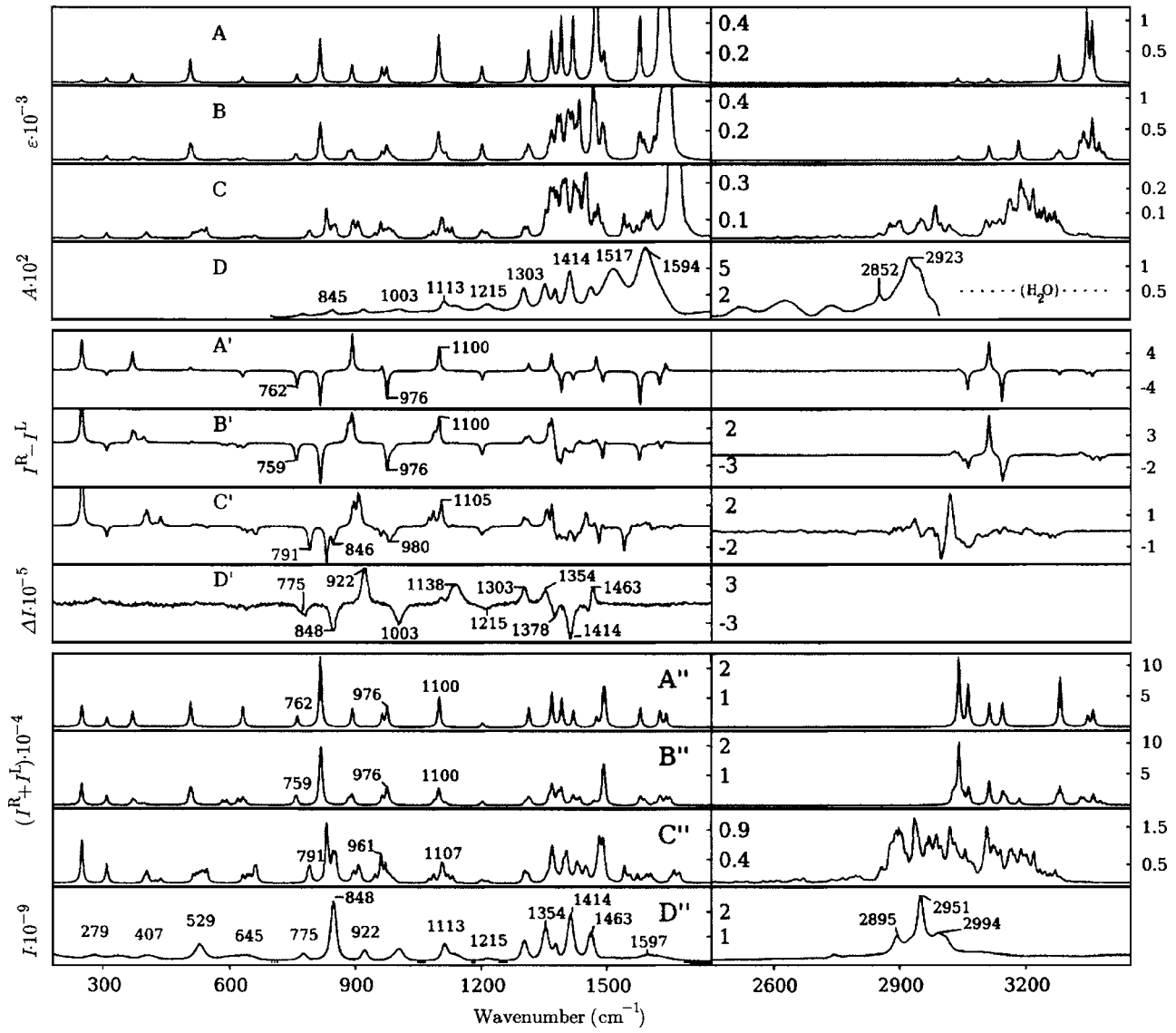


FIG. 7. The effect of the Boltzmann conformer averaging on absorption (A–D), ROA (A′–D′), and Raman (A″–D″) alanine spectra: harmonic approximation for the equilibrium geometry (A, A′, and A″), conformer averaging of harmonic (B, B′, and B″), and anharmonic (C, C′, and C″) spectra for the structures defined in Fig. 6. The experimental IR absorbance (D) was measured by the ATR technique. The experimental ROA (D′) and Raman (D″) spectra are taken from Ref. 2. The simulations were done for the temperature of 300 K at the B3LYP/CPCM/6-31++$G^{**}$ level, using 5000 VCI states with three low-frequency modes frozen.

### E. Spectra averaging

In order to judge the effect of the anharmonic corrections, it is important to estimate all other factors that may contribute to the spectra with the same magnitude, including molecular flexibility and temperature averaging. For proline and alanine, at least two lowest-energy modes have to be averaged in room temperature.[2,10] In Fig. 6 we reproduce relative probability distributions obtained with the B3LYP/CPCM/6-31++$G^{**}$ energy surfaces. 7 (for alanine) and 11 (for proline) conformations visible as the triangles in Fig. 6 were taken in the averaging. A more complete sampling of the conformer space, as could be done at the harmonic limit,[2,10] was prohibited by the time needed to calculate the anharmonic terms. However, with a balanced selection of the conformers the extent of the averaging changes could also be estimated for the anharmonic case. Particularly, Figs. 7 and 8 compare absorption (traces A–D), ROA (A′–D′), and Raman (A″–D″) alanine and proline spectra simulated at the harmonic level for rigid molecules (A, A′, and A″) with the harmonic (B, B′, and B″) and anharmonic (C, C′, and C″) averages, together with the experiments (D, D′, and D″).

The harmonic and anharmonic averages in the absorption spectra (B and C in Figs. 7 and 8) are quite similar below 800 $cm^{-1}$; this region, however, is not accessible experimentally. A maximum absorption intensity within 800–1800 $cm^{-1}$ is mostly associated with the movement of the polar groups ($NH_3^+$, $NH_2^+$, and $CO_2^-$). This is not a favorable situation for the modeling, because such harmonic frequencies are calculated with the biggest error due to the interaction with the solvent. The experimental C—O stretching signal is strongly mixed with the water absorption and the base line subtraction may have somewhat affected the apparent frequencies and intensities of the corresponding

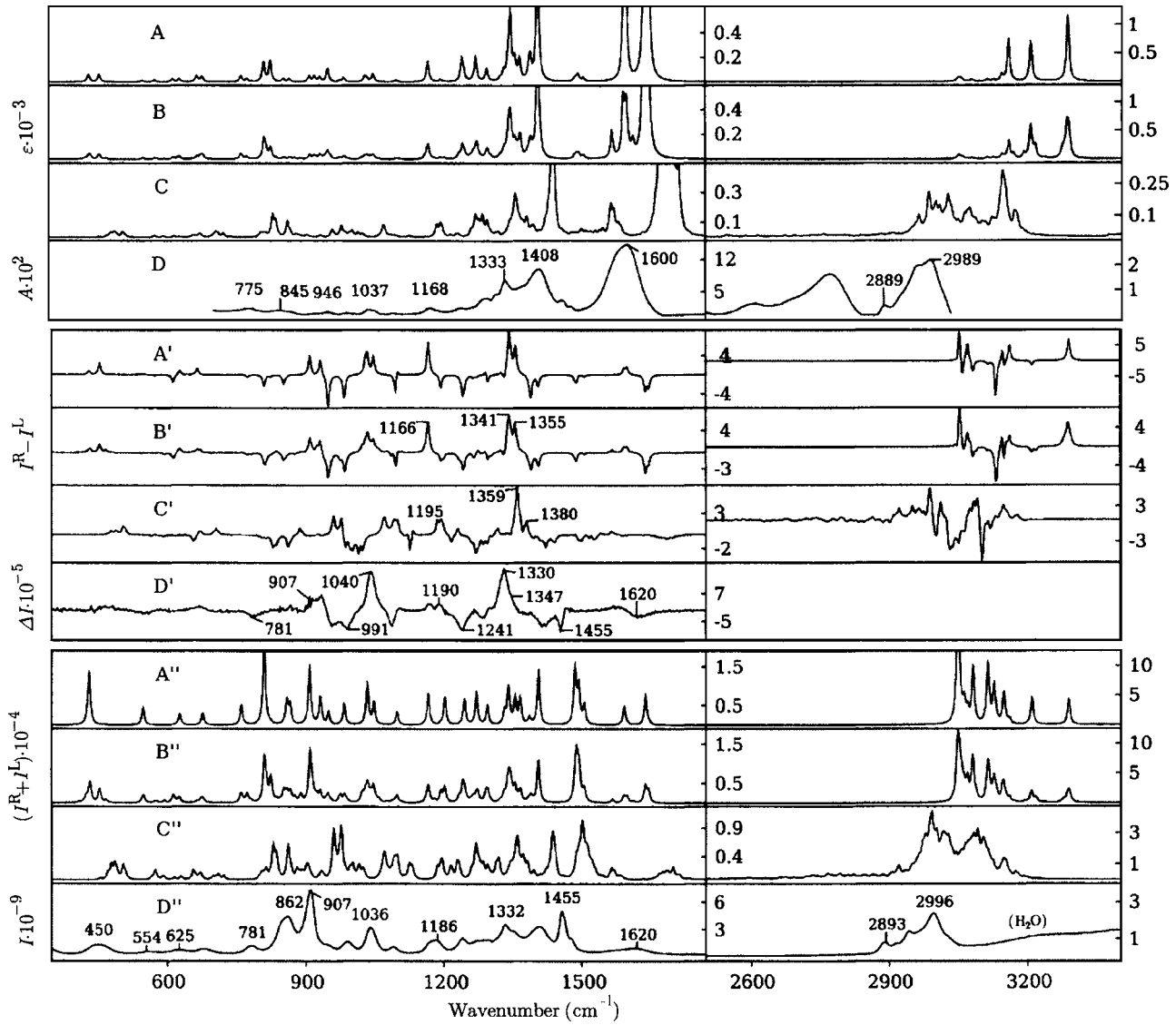


FIG. 8. The effect of Boltzmann conformer averaging on absorption (A–D), ROA (A′–D′), and Raman (A″–D″) proline spectra. The layout of the figure is analogous to Fig. 7: harmonic approximation (A, A′, and A″, average of the A+B conformers in Fig. 1), Boltzmann-weighted conformer averaging (Fig. 6) of the harmonic (B, B′, and B″), and anharmonic (C, C′, and C″) spectra (300 K, B3LYP/CPCM/6-31++$G^{**}$, 5000 VCI states, five modes frozen). The experimental absorption spectrum (D) was measured by the ATR technique; the experimental ROA (D′) and Raman (D″) spectra are taken from Ref. 10.

IR bands at 1594 and 1599 $cm^{-1}$ for alanine and proline, respectively. Similarly, the water absorption and the broad N–H stretching signal may obscure the region above 2500 $cm^{-1}$ with the very weak C–H stretching signal. Nevertheless, the averaged anharmonic C–H stretching frequencies (2900–3100 $cm^{-1}$) are clearly superior to the harmonic simulations, although detailed absorption profile cannot be compared. Within 2500–2850 $cm^{-1}$ we can see a relatively strong signal, particularly in the proline absorption spectrum, which we currently cannot explain. Same spectral features were also observed in an optical cell; only the attentuated total reflection (ATR) measurements, however, are shown because of the extended available frequency range. The N–H stretching signal($\sim >$3000 $cm^{-1}$) (Ref. 55) is most affected by the hydrogen bonding and cannot be identified in the IR experiment at all. In Raman scattering, the NH stretching contribution is identifiable, but very weak and broad.

For the Raman and ROA intensities most of the positive effects of the anharmonic corrections discussed above for the rigid geometries also persist after the averaging. In the lower wave number region, for example, we can see improved alanine frequency of the 759/791/775 $cm^{-1}$ band (harmonic average/anharmonic average/experiment, traces B″/C″/D″ in Fig. 7), new peak at 846 $cm^{-1}$ (trace C′, experimentally detectable as a weak negative ROA shoulder at 861 $cm^{-1}$, trace D′), improved frequency and relative intensity of the 976/980/1003 $cm^{-1}$ band, and more realistic relative intensities of the 1087–1100 (harm) /1085–1105 (anharm) /1104–1140 $cm^{-1}$ ROA and Raman bands. As pointed out above, the region of 1300–1550 $cm^{-1}$ is difficult to simulate. We can only conclude that the anharmonic forces play a substantial role at the coupling of involved vibrations and the anharmonic corrections improve a general ROA and Raman intensity profile, if compared with the harmonic case, but a band-to-band comparison is not possible. The same is also true for the C–H stretching Raman signal at 2900–3100 $cm^{-1}$. Simi-

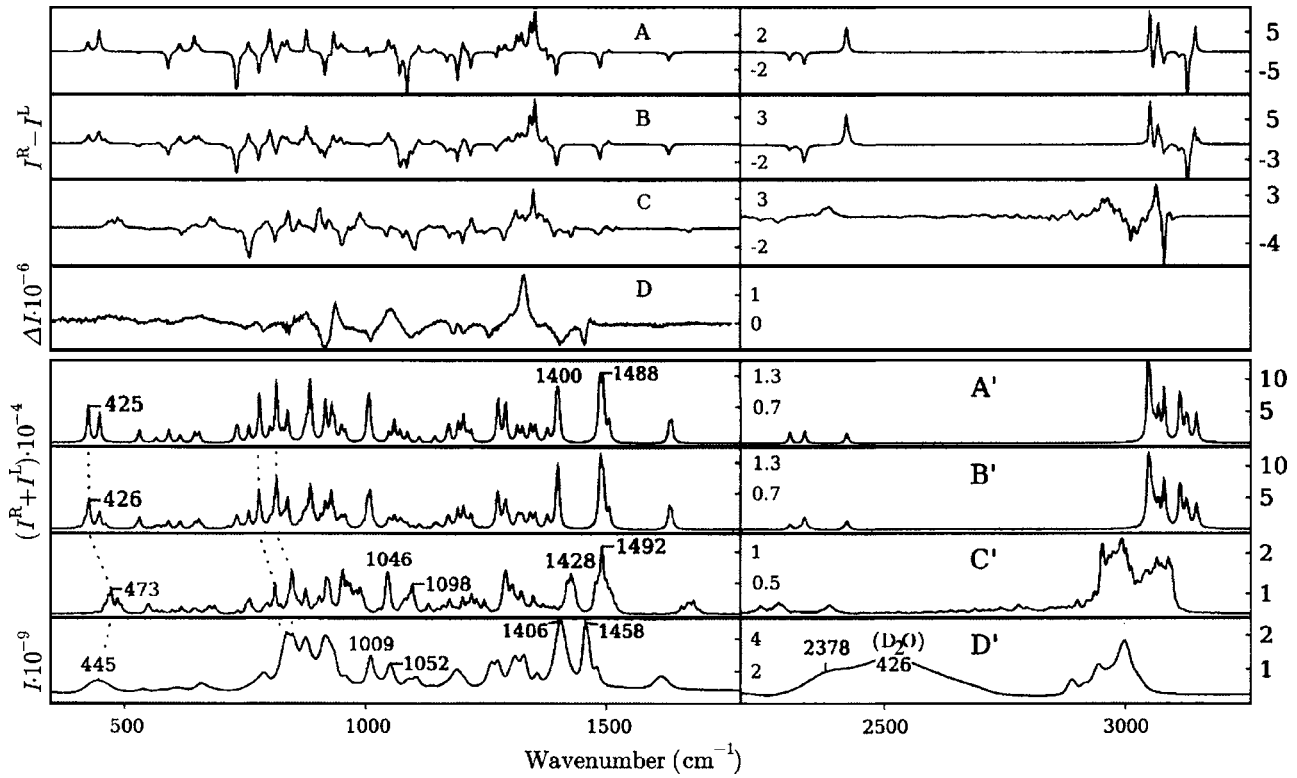


FIG. 9. Harmonic (A and A′), Boltzmann-averaged harmonic (B and B′), and VCI (C and C′, for 300 K, B3LYP/CPCM/6-31++$G^{**}$, 5000 VCI states, five modes frozen) Raman (A–D) and ROA (A′–D′) spectra for deuterated ($ND_3^+$) proline, A+B conformer average. The experimental spectrum in $D_2O$ (D and D′) was taken from Ref. 10.

lar situation appears for the proline spectra (Fig. 8). Here, the anharmonic averaged simulation provides a reasonable agreement with the experiment even in the ~1205–1550 cm$^{-1}$ region, which was found difficult for alanine: the shapes, frequencies, and intensities of the ROA bands (trace C′) become more realistic. For example, the harmonic positive ROA band pair (1166 cm$^{-1}$, trace B′) splits and the intensity decreases in C′ (1186–1195 cm$^{-1}$), in favor of experimental values of 1167–1190 cm$^{-1}$, the positive harmonic doublet (trace B′, 1341–1355 cm$^{-1}$) changes to the dominant single band at 1359 cm$^{-1}$ with a shoulder at 1380 cm$^{-1}$ in C′, similarly as seen in the experimental spectrum D′ (1330, shoulder 1347 cm$^{-1}$).

Similar extent of the anharmonic forces can be observed in the Raman and ROA spectra of deuterated ($ND_2^+$) proline plotted in Fig. 9. One might expect that the deuterated species would behave "more harmonic" as heavy atoms move less from their equilibrium positions ($\langle x^2 \rangle \propto 1/\sqrt{m}$) and sample less of the potential landscape. This is difficult to prove here because all simulations still significantly deviate from the experimental spectra. However, individual positive effects of the anharmonic forces in the spectra can be found, similarly as for the nondeuterated species. Most notably, the splitting of the harmonic bands at 1400 and 1488 cm$^{-1}$ decreases (shifting them to 1428 and 1492 cm$^{-1}$ in trace C′, Fig. 9) and better corresponds to the observed values of 1406 and 1458 cm$^{-1}$. Consequently, the overall anharmonic ROA pattern within ~1300–1500 cm$^{-1}$ (trace C) seems to be slightly better in comparison with the harmonic simulation B. Moreover, the relative intensity of the Raman bands observed experimentally (D′) at 1009 and 1052 cm$^{-1}$ improves due to the anharmonicities (at 1046 and 1098 cm$^{-1}$ in C′) as the higher-frequency band becomes stronger. All simulations provide reasonable frequencies of the N–D stretching bands, visible probably as a shoulder at ~2378 cm$^{-1}$ on the heavy water (incompletely subtracted) O–D stretching signal[55] in D′.

## IV. CONCLUSIONS

For the alanine and proline zwitterions we have applied the VSCF, PT2, and VCI anharmonic corrections in simulations of the Raman, ROA, and absorption spectra and analyzed their agreement with the experiment. The VSCF and PT2 methods did not provide convincing improvement of spectral shapes and frequencies except for the C–H stretching region. On the other hand, the VCI correction clearly improved the Raman and ROA spectral intensities, including the vibrations of 200–1800 cm$^{-1}$. Within 1205–1550 cm$^{-1}$ the improvement still did not enable to assign all experimental features due to the high density of vibrational states (mostly C–H bending) and coupling to the motion of the polar groups strongly interacting with the environment. In spite of the limitations, we consider inclusion of the anharmonic effects to be an important step in the continuous effort to make interpretation of the vibrational spectra more accurate, which will lead to better understanding of molecular structure, dynamics, and interactions.

## ACKNOWLEDGMENTS

The work was supported by the Grant Agency of the Czech Republic (Grant Nos. 203/06/0420 and 202/07/0732), Grant Agency of the Academy of Sciences (A400550702), Grand Agency of the Charles University (19707), and by the Ministry of Education, Youth and Sports of the Czech Republic (MSM 0021620835).

[1] L. D. Barron, L. Hecht, and A. D. Bell, in *Circular Dichroism and the Conformational Analysis of Biomolecules*, edited by G. D. Fasman (Plenum, New York, 1996), p. 653; L. A. Nafie, in *Modern Nonlinear Optics*, edited by M. Evans and S. Kielich (Wiley, New York, 1994), Vol. 85, pt. 3, p. 105; L. D. Barron, S. J. Ford, A. D. Bell, G. Wilson, L. Hecht, and A. Cooper, Faraday Discuss. **99**, 217 (1994); K. J. Jalkanen, R. M. Nieminen, M. Knapp-Mohammady, and S. Suhai, Int. J. Quantum Chem. **92**, 239 (2003); J. Kapitán, V. Baumruk, V. Kopecký, Jr., and P. Bouř, J. Am. Chem. Soc. **128**, 2438 (2006); K. Ruud, T. Helgaker, and P. Bouř, J. Phys. Chem. A **106**, 7448 (2002).
[2] J. Kapitán, V. Baumruk, V. Kopecký, Jr., and P. Bouř, J. Phys. Chem. A **110**, 4689 (2006).
[3] L. D. Barron and A. D. Buckingham, Mol. Phys. **20**, 1111 (1971).
[4] L. D. Barron, M. P. Bogaard, and A. D. Buckingham, J. Am. Chem. Soc. **95**, 603 (1973); W. Hug, S. Kint, G. F. Bailey, and J. R. Schere, *ibid.* **97**, 5589 (1975).
[5] P. L. Polavarapu, Angew. Chem., Int. Ed. **41**, 4544 (2002).
[6] L. D. Barron, L. Hecht, I. H. McColl, and E. W. Blanch, Mol. Phys. **102**, 731 (2004); F. Zhu, N. W. Isaacs, L. Hecht, and L. D. Barron, J. Am. Chem. Soc. **127**, 6142 (2005); E. W. Blanch, I. H. McColl, L. Hecht, K. Nielsen, and L. D. Barron, Vib. Spectrosc. **35**, 87 (2004); L. A. Nafie, G. S. Yu, and T. B. Freedman, *ibid.* **8**, 231 (1995); J. Kapitán, V. Baumruk, V. Gut, J. Hlaváček, H. Dlouhá, M. Urbanová, E. Wunsch, and P. Maloň, Collect. Czech. Chem. Commun. **70**, 403 (2005); P. Bouř, M. Buděšínský, V. Špirko, J. Kapitán, J. Šebestík, and V. Sychrovský, J. Am. Chem. Soc. **127**, 17079 (2005).
[7] C. N. Tam, P. Bouř, and T. A. Keiderling, J. Am. Chem. Soc. **118**, 10285 (1996).
[8] C. Toniolo, F. Formaggio, S. Tognon *et al.*, Biopolymers **75**, 32 (2004); E. W. Blanch, A. C. Gill, A. G. O. Rhie, J. Hope, L. Hecht, K. Nielsen, and L. D. Barron, J. Mol. Biol. **343**, 467 (2004).
[9] P. Bouř, V. Sychrovský, P. Maloň, J. Hanzlíková, V. Baumruk, J. Pospíšek, and M. Buděšínský, J. Phys. Chem. A **106**, 7321 (2002).
[10] J. Kapitán, V. Baumruk, V. Kopecký, Jr., R. Pohl, and P. Bouř, J. Am. Chem. Soc. **128**, 13451 (2006).
[11] C. E. Blom and C. Altona, Mol. Phys. **31**, 1377 (1976).
[12] P. Pulay, J. Phys. Chem. **99**, 3093 (1995).
[13] H. Romanowski, J. M. Bowman, and L. B. Harding, J. Chem. Phys. **82**, 4155 (1985); A. E. Roitberg and R. B. Gerber, J. Phys. Chem. B **101**, 1700 (1997).
[14] J. O. Jung and R. B. Gerber, J. Chem. Phys. **105**, 10332 (1996).
[15] G. Rauhut, J. Chem. Phys. **121**, 9313 (2004).
[16] S. Carter, J. M. Bowman, and N. C. Handy, Theor. Chem. Acc. **53**, 1179 (1997).
[17] W. Schneider and W. Thiel, Chem. Phys. Lett. **157**, 367 (1989); P. Bouř and L. Bednárová, J. Phys. Chem. **99**, 5961 (1994); V. Barone, J. Chem. Phys. **122**, 014108 (2005).
[18] D. Papoušek and M. R. Aliev, *Molecular Vibrational/Rotational Spectra* (Academia, Prague, 1982).
[19] J. M. Bowman, J. Chem. Phys. **68**, 608 (1978).
[20] K. M. Christoffel and J. M. Bowman, Chem. Phys. Lett. **85**, 220 (1982).
[21] S. Carter, J. M. Bowman, and N. C. Handy, Theor. Chem. Acc. **100**, 191 (1998).
[22] O. Christiansen, J. Chem. Phys. **120**, 2149 (2004).
[23] R. B. Gerber and M. A. Ratner, Chem. Phys. Lett. **68**, 195 (1979).
[24] L. S. Norris, M. A. Ratner, A. E. Roitberg, and R. B. Gerber, J. Chem. Phys. **105**, 11261 (1996).
[25] P. Daněček and P. Bouř, J. Comput. Chem. **28**, 1617 (2007).
[26] N. Matsunaga, G. M. Chaban, and R. B. Gerber, J. Chem. Phys. **117**, 3541 (2002).
[27] L. D. Barron, *Molecular Light Scattering and Optical Activity* (Cambridge University Press, Cambridge, 2004).
[28] P. L. Polavarapu, *Vibrational Spectra: Principles and Applications with Emphasis on Optical Activity* (Elsevier, Amsterdam, 1998); L. A. Nafie and C. G. Zimba, in *Biological Applications of Raman Spectroscopy*, edited by T. G. Spiro (Wiley, New York, 1987), Vol. 1, p. 307; L. A. Nafie and T. B. Freedman, in *Circular Dichroism: Principles and Applications*, 2nd ed., edited by N. Berova, K. Nakanishi, and R. W. Woody (Wiley-VCH, New York, 2000).
[29] M. J. Frisch, G. W. Trucks, H. B. Schlegel *et al.*, GAUSSIAN 03, Revision C.02, Gaussian, Inc., Wallingford, CT, 2004.
[30] C. C. J. Roothan, Rev. Mod. Phys. **23**, 69 (1951).
[31] C. Møller and M. S. Plesset, Phys. Rev. **46**, 618 (1934).
[32] A. Becke, Phys. Rev. A **38**, 3098 (1988).
[33] C. Adamo and V. Barone, J. Chem. Phys. **108**, 664 (1998).
[34] A. D. Becke, J. Chem. Phys. **104**, 1040 (1996).
[35] A. D. Becke, J. Chem. Phys. **98**, 5648 (1993).
[36] J. P. Perdew, Phys. Rev. B **33**, 8822 (1986).
[37] J. P. Perdew, K. Burke, and Y. Wang, Phys. Rev. B **54**, 16533 (1996).
[38] J. P. Perdew, K. Burke, and M. Ernzerhof, Phys. Rev. Lett. **77**, 3865 (1996).
[39] H. L. Schmider and A. D. Becke, J. Chem. Phys. **108**, 9624 (1998).
[40] F. A. Hamprecht, A. J. Cohen, D. J. Tozer, and N. C. Handy, J. Chem. Phys. **109**, 6264 (1998).
[41] T. van Voorhis and G. E. Scuseria, J. Chem. Phys. **109**, 400 (1998).
[42] N. C. Handy and A. J. Cohen, Mol. Phys. **99**, 403 (2001).
[43] R. G. Parr and W. Yang, *Density-Functional Theory of Atoms and Molecules* (Oxford University Press, New York, 1994).
[44] J. C. Slater, *The Self-Consistent Field for Molecular and Solids* (McGraw-Hill, New York, 1974).
[45] K. Burke, J. P. Perdew, and Y. Wang, *Electronic Density Functional Theory: Recent Progress and New Directions* (Plenum, New York, 1998).
[46] P. M. W. Gill, Mol. Phys. **89**, 433 (1996).
[47] C. Lee, W. Yang, and R. G. Parr, Phys. Rev. B **37**, 785 (1988).
[48] A. Klamt, in *The Encyclopedia of Computational Chemistry*, edited by P. R. Schleyer, N. L. Allinger, T. Clark, J. Gasteiger, P. A. Kollman, H. F. Schaefer III, and P. R. Schreiner (Wiley, Chichester, 1998), Vol. 1, p. 604.
[49] M. Reiher, V. Liegeois, and K. Ruud, J. Phys. Chem. A **109**, 7567 (2005).
[50] E. B. Wilson, J. C. Decius, and P. C. Cross, *Molecular Vibrations* (Dover, New York, 1980).
[51] P. Bouř, J. McCann, and H. Wieser, J. Phys. Chem. A **102**, 102 (1998); A. P. Scott and L. Radom, J. Phys. Chem. **100**, 16502 (1996).
[52] P. Bouř and T. A. Keiderling, J. Phys. Chem. B **109**, 23687 (2005); J. Kubelka, R. Huang, and T. A. Keiderling, *ibid.* **109**, 8231 (2005); P. Bouř, J. Kubelka, and T. A. Keiderling, Biopolymers **65**, 45 (2002).
[53] D. Begue, A. Benidar, and C. Pouchan, Chem. Phys. Lett. **430**, 215 (2006).
[54] O. Christiansen and J. M. Luis, Int. J. Quantum Chem. **104**, 667 (2005).
[55] M. Horák and D. Papoušek, *Infračervená Spektra a Struktura Molekul* (Academia, Prague, 1976).